Juno, the angular momentum of Jupiter and the Lense-Thirring effect

Lorenzo Iorio

INFN-Sezione di Pisa. Permanent address for correspondence: Viale Unità di Italia 68, 70125, Bari (BA), Italy. E-mail: lorenzo.iorio@libero.it

ABSTRACT

The recently approved Juno mission will orbit Jupiter for one year in a highly eccentric ($r_{\mathrm{min}} = 1.06R_{\mathrm{Jup}}$, $r_{\mathrm{max}} = 39R_{\mathrm{Jup}}$) polar orbit ($i = 90$ deg) to accurately map, among other things, the jovian magnetic and gravitational fields. Such an orbital configuration yields an ideal situation, in principle, to attempt a measurement of the general relativistic Lense-Thirring effect through the Juno's node Ω which would be displaced by about 570 m over the mission's duration. Conversely, by assuming the validity of general relativity, the proposed test can be viewed as a direct, dynamical measurement of the Jupiter's angular momentum S which would give important information concerning the internal structure and formation of the giant planet. The long-period orbital perturbations due to the zonal harmonic coefficients $J_\ell, \ell = 2, 3, 4, 6$ of the multipolar expansion of the jovian gravitational potential accounting for its departures from spherical symmetry are, in principle, a major source of systematic bias. While the Lense-Thirring node rate is independent of the inclination i, the node zonal perturbations vanish for $i = 90$. In reality, the orbit injection errors will induce departures δi from the ideal polar geometry, so that, according to a conservative analytical analysis, the zonal perturbations may come into play at an unacceptably high level, in spite of the expected improvements in the low-degree zonals by Juno. A linear combination of Ω, the periJove ω and the mean anomaly $\mathcal{M}$ cancels out the impact of J_2 and J_6. A two orders of magnitude improvement in the uncanceled J_3 and J_4 would be needed to reduce their bias on the relativistic signal to the percent level; it does not seem unrealistic because the expected level of improvement in such zonals is three orders of magnitude. More favorable conclusions are obtained by looking at single Doppler range-rate measurements taken around the closest approaches to Jupiter; numerical simulations of the classical and gravito-magnetic

signals for this kind of observable show that a $0.2 - 5\%$ accuracy would be a realistic goal.

Subject headings: Relativity and gravitation; Lunar, planetary, and deep-space probes; Jupiter; Gravitational fields

1.   Introduction

Recently, NASA approved the Juno[1] mission (Matousek 2007) to Jupiter. Juno is a spinning, solar powered spacecraft to be placed in a highly eccentric polar orbit around Jupiter (see Table 1 for its relevant orbital parameters) specifically designed to avoid its highest radiation regions. Understanding the formation, evolution and structure of Jupiter is the primary science goal of Juno. It will carry onboard a dual frequency

Table 1: Planetocentric nominal orbital parameters of Juno. a, e, i are the semi-major axis (in jovian radii $R = 71492$ km), the eccentricity and the inclination (in deg) to the Jupiter's equator, respectively. P is the orbital period (in days). T is the mission duration (in years).

a (R)	e	i (deg)	P (d)	T (yr)
20.03	0.947	90	11	1

gravity/radio science system, a six wavelength microwave radiometer for atmospheric sounding and composition, a dual-technique magnetometer, plasma detectors, energetic particle detectors, a radio/plasma wave experiment, and an ultraviolet imager/spectrometer. The nominal mission's lifetime is 1 year. Juno is aimed, among other things, at accurately mapping the gravitational field of Jupiter (Anderson 1976) with unprecedented accuracy (Anderson et al. 2004) by exploiting the slow apsidal precession of its 11-day orbit.

In this paper we wish to explore the possibility offered by Juno to perform a test of general relativity by directly measuring the gravito-magnetic Lense-Thirring effect; its basics are reviewed below. Even putting aside the more or less successful attempts so far performed with other natural and artificial test particles orbiting different central bodies, it must be recalled that a satisfactorily empirical corroboration of a fundamental theory like

[1]See on the WEB http://juno.wisc.edu/index.html

general relativity requires that as many independent experiments as possible are conducted by different scientists in different laboratories; thus, it is worthwhile to try to use different gravitational fields to perform such a test of intrinsic gravito-magnetism. Conversely, since, as we will see, the Lense-Thirring precessions are due to the proper angular momentum $\boldsymbol{S}$ of the orbited central body, one may also assume the existence of the general relativistic gravito-magnetism and consider such a test as a direct, dynamical measurement of the Jupiter's angular momentum through the Lense-Thirring effect; this would yield further, important information concerning the interior of Jupiter. Indeed, the moment of inertia ratio C/MR^2 entering S is a measure of the concentration of mass towards the center of the planet (Irwin 2003). Such a figure, together with the measured values of the zonal[2] coefficients of the gravity field accounting for its deviations from spherical symmetry may be fitted with internal models that model how the density, pressure, temperature and composition vary with depth (Irwin 2003; Guillot 2005; Hori et al. 2008). Moreover, a dynamical, model-independent determination of S would be important also for a better knowledge of the history and formation of Jupiter (Machida et al. 2008).

Let us, now, briefly review the basics of the Lense-Thirring effect (Lense and Thirring 1918; Zel'dovich and Novikov 1971; Soffel 1989). In its weak-field and slow-motion approximation, the field equations of general relativity get linearized looking like those of the Maxwellian electromagnetism. Analogously with the magnetic field generated by moving electric charges, mass-energy currents give rise to a gravito-magnetic field $\boldsymbol{B}_{\mathrm{g}}$ (Mashhoon 2007); far from an isolated spinning body of mass M and proper angular momentum $\boldsymbol{S}$ it is (Lichtenegger and Iorio 2007)

$$\boldsymbol{B}_{\mathrm{g}} = -\frac{G}{cr^3}\left[\boldsymbol{S} - 3\left(\boldsymbol{S}\cdot\hat{\boldsymbol{r}}\right)\hat{\boldsymbol{r}}\right], \tag{1}$$

where G is the Newtonian gravitational constant and c is the speed of light in vacuum. $\boldsymbol{B}_{\mathrm{g}}$

---

[2]They preserve the axial symmetry.

exerts the non-central Lorentz-like acceleration (Soffel 1989; Mashhoon 2007)

$$\boldsymbol{A}^{\mathrm{GM}} = -\frac{2}{c}\boldsymbol{v} \times \boldsymbol{B}_{\mathrm{g}} \tag{2}$$

upon a test particle moving with velocity $\boldsymbol{v}$. For ordinary astronomical bodies like, e.g., a planet, A^{GM} is many orders of magnitude smaller than the Newtonian monopole $A^{\mathrm{N}} = GM/r^2$, so that it can be considered as a small perturbation. As a result, the longitude of the ascending node Ω and the argument of pericentre ω of a test particle undergo small secular precessions (Lense and Thirring 1918)

$$\dot{\Omega}_{\mathrm{LT}} = \frac{2GS}{c^2 a^3 (1 - e^2)^{3/2}}, \tag{3}$$

$$\dot{\omega}_{\mathrm{LT}} = -\frac{6GS\cos i}{c^2 a^3 (1 - e^2)^{3/2}}. \tag{4}$$

Concerning a direct measurement of the Lense-Thirring effect, attempts have been recently performed with the LAGEOS satellites in the gravitational field of the Earth (Cugusi and Proverbio 1978; Ciufolini and Pavlis 2004; Ries et al. 2008), the Mars Global Surveyor probe orbiting Mars (Iorio 2006, 2009a) and some of the inner planets of the Solar System (Iorio 2008). The evaluation of the total accuracy of the LAGEOS (Ciufolini and Pavlis 2005; Iorio 2007a) and MGS (Krogh 2007; Iorio 2009a) tests has raised a debate in the recent past because of the difficulty of realistically assessing the impact of certain competing dynamical effects acting as sources of systematic errors; for example, the total accuracy of the LAGEOS test may be as large as some tens percent (Iorio 2009b); similar shortcomings may affect also the approved LARES mission (Iorio 2009c,d). For an overview of several theoretical and experimental features of gravito-magnetism see, e.g., (Iorio 2007b). Concerning the jovian scenario, Lense and Thirring (1918) originally proposed to use the orbital precessions of the Galilean satellites; such a possibility has been recently investigated by Iorio and Lainey (2005), but it seems to be still premature. Haas and Ross (1975) proposed a spacecraft-based experiment in the gravitational field of

Jupiter to measure another gravito-magnetic effect, i.e. the precession of a gyroscope (Pugh 1959; Schiff 1960). It is also one of the goals of the GP-B mission (Everitt 1974) whose target was a $\approx 1\%$ measurement of such an effect with four superconducting gyroscopes carried onboard by a low-altitude polar spacecraft in the gravitational field of the Earth, but it is still unclear if it will be finally possible to meet the original accuracy because of some unexpected systematic aliasing effects occurred during the mission[3] (Conklin et al. 2008; Everitt et al. 2009). A test of gravito-magnetism[4] concerning the deflection of electromagnetic waves by Jupiter in its orbital motion has been performed in a dedicated radio-interferometric experiment (Fomalont and Kopeikin 2008). With regard to other suggested non-gravito-magnetic tests of general relativity in the jovian gravitational field, Hiscock and Lindblom (1979) proposed to measure the much larger gravito-electric Einstein pericenter precessions (Einstein 1915) of the natural satellites of Jupiter and Saturn. There exist also plans for performing a test of the light bending due to the Jupiter's monopole and quadrupole mass moments with the forthcoming astrometric mission GAIA (Crosta and Mignard 2006).

The Jupiter's proper angular momentum amounts to (Soffel et al. 2003)

$$S \approx 6.9 \times 10^{38} \text{ kg m}^2 \text{ s}^{-1}. \tag{5}$$

---

[3]See on the WEB http://einstein.stanford.edu/

[4]In this case, the mass currents inducing a gravito-magnetic action are not those related to the Jupiter's proper rotation (intrinsic gravito-magnetism), but are due to its translational orbital motion (extrinsic gravito-magnetism).

Table 1 and eq. (5) yield for Juno

$$\dot{\Omega}_{\text{LT}} = 68.5 \text{ mas yr}^{-1} \tag{6}$$

$$\dot{\omega}_{\text{LT}} = 0. \tag{7}$$

which correspond to a shift $\Delta\nu$ of the cross-track component of the planetocentric position (Christodoulidis et al. 1988)

$$\Delta\nu_{\text{LT}} = a\sqrt{1 + \frac{e^2}{2}} \sin i \Delta\Omega_{\text{LT}} = 572 \text{ m } (T = 1 \text{ yr}) \tag{8}$$

over the entire duration of the mission. A total accuracy of the order of 1-10 m with respect to the km-level of the past Jupiter missions in reconstructing the Juno's orbit in a planetocentric frame does not seem an unrealistic target, although much work is clearly required in order to have a more firm answer. Note that a 1-10 m accuracy implies a $0.2 - 2\%$ error in measuring the gravito-magnetic shift

The fact that the possibility of detecting the Lense-Thirring effect with Juno's orbit seems worth of further consideration can be preliminarily shown also with a different approach with respect to the cumulative measurement over the full mission duration previously outlined. Indeed, a gravity-science pass for Juno is defined by a continuous, coherent Doppler range-rate measurement plus and minus three hours of closest approach; in practice, most of the Lense-Thirring precession takes place just during such a six-hours pass, a near optimum condition. Another crucial factor is the orientation of the Earth to the Juno's orbit: our planet will be aligned 67 deg from the probe's orbital plane at approximately two degrees south latitude on the jovian equator. Preliminary numerical simulations of the Juno's Lense-Thirring Doppler range-rate signal show that such an orbital geometry represent a perfect compromise for measuring both the Jupiter's even zonal harmonics and the gravitomagnetic signal itself. Indeed, it turns out that the maximum

Lense-Thirring Doppler signal over a single six-hour gravity pass is of the order of hundred μm s^{-1}, while the limit of accuracy for Juno's Ka-band Doppler system is about one μm s^{-1} over such a pass. Thus, even by taking 25 repeated passes, over a total of approximately 33, it would be possible to reach a measurement precision below the percent level.

Concerning the magnitude of the jovian gravito-magnetic field, it must be noted that in literature there are estimates for S which point towards smaller values than eq. (5) by a factor $1.5 - 1.6$; for example, Machida et al. (2008) yield

$$S = 4.14 \times 10^{38} \text{ kg m}^2 \text{ s}^{-1}; \tag{9}$$

the ratio of eq. (5) to eq. (9), i.e. 1.6, is close to 1.5 coming from the ratio of $C/MR^2 = 2/5 = 0.4$, valid for a homogenous sphere, to $C/MR^2 = 0.264$ by Irwin (2003) who assumes a concentration of mass towards the Jupiter's center. Here we will consider only the systematic uncertainty induced by the imperfect knowledge of the Newtonian part of the Jupiter's gravitational field; we will use eq. (5) for S.

2. The systematic uncertainty due to the zonal harmonics of the Jupiter's gravitational potential

A major source of systematic uncertainty is represented, in principle, by the departures of the Jupiter's gravitational field from spherical symmetry (Anderson 1976).

2.1. Analytical calculations

Indeed, the zonal ($m = 0$) harmonic coefficients J_ℓ of the multipolar expansion of the Newtonian part of the planet's gravitational potential give rise to long-period, that is averaged over one orbital revolution, orbital effects on the longitude of the ascending node

Ω, the argument of pericentre ω and the mean anomaly $\mathcal{M}$ (Kaula 1966)

$$\left\langle \dot{\Omega} \right\rangle = \sum_{\ell=2} \dot{\Omega}_{.\ell} J_\ell, \tag{10}$$

$$\left\langle \dot{\omega} \right\rangle = \sum_{\ell=2} \dot{\omega}_{.\ell} J_\ell, \tag{11}$$

$$\left\langle \dot{\mathcal{M}} \right\rangle = \sum_{\ell=2} \dot{\mathcal{M}}_{.\ell} J_\ell, \tag{12}$$

$$\tag{13}$$

where $\dot{\Omega}_{.\ell}, \dot{\omega}_{.\ell}, \dot{\mathcal{M}}_{.\ell}$ are coefficients depending on the planet's GM and equatorial radius R, and on the spacecraft's inclination i and eccentricity e through the inclination $F_{\ell mp}(i)$ and eccentricity $G_{\ell pq}(e)$ functions, respectively (Kaula 1966). Note that one of the major scientific goals of the Juno mission is a greatly improved determination of just the harmonic coefficients of the jovian gravity potential; for the present-day values of the zonals[5] for $\ell = 2, 3, 4, 6$ see Table 2. According to Anderson et al. (2004), it might be possible to

Table 2: Zonal harmonics of the Jupiter's gravity field according to the JUP230 orbit solution (Jacobson 2003).

J_2 ($\times 10^6$)	J_3 ($\times 10^6$)	J_4 ($\times 10^6$)	J_6 ($\times 10^6$)
14696.43 ± 0.21	-0.64 ± 0.90	-587.14 ± 1.68	34.25 ± 5.22

determine the first three even zonals with an accuracy of 10^{-9} and the other ones up to $\ell = 30$ at a 10^{-8} level. Concerning J_2, this would be an improvement of two orders of

---

[5]The Jupiter gravity field is essentially determined by the Pioneer 11 flyby at $1.6 R_{\mathrm{Jup}}$ (Anderson 1976); Voyager added little, and Galileo, which never got close to Jupiter, added nothing.

magnitude with respect to Table 2, while the improvements in J_4 and J_6 would be of the order of three orders of magnitude. By using the results we are going to present below for the long-period node and pericenter precessions, it can be shown that determining the low degree zonals at 10^{-9} level of accuracy translates into an accuracy of the order of $0.5 - 1$ mas yr^{-1} in $\dot{\Omega}$ and $\dot{\omega}$, thus confirming the expectations of the previous Section.

For the long-period terms the condition

$$\ell - 2p + q = 0 \tag{14}$$

is fulfilled. Thus,

$$\dot{\Omega}_{.\ell} = -\frac{n}{\sqrt{1-e^2}\sin i}\left(\frac{R}{a}\right)^\ell \sum_{p=0}^\ell \left[\frac{dF_{\ell 0 p}}{di}G_{\ell p(2p-\ell)}W_{\ell 0 p(2p-\ell)}\right], \tag{15}$$

$$\dot{\omega}_{.\ell} = -\frac{n}{\sqrt{1-e^2}}\left(\frac{R}{a}\right)^\ell \sum_{p=0}^\ell \left[-\cot i\frac{dF_{\ell 0 p}}{di}G_{\ell p(2p-\ell)} + \frac{(1-e^2)}{e}F_{\ell 0 p}\frac{dG_{\ell p(2p-\ell)}}{de}\right]W_{\ell 0 p(2p-\ell)}, \tag{16}$$

$$\dot{\mathcal{M}}_{.\ell} = n\left\{1 - \left(\frac{R}{a}\right)^\ell \sum_{p=0}^\ell F_{\ell 0 p}\left[6G_{\ell p(2p-\ell)} - \frac{(1-e^2)}{e}\frac{dG_{\ell p(2p-\ell)}}{de}\right]W_{\ell 0 p(2p-\ell)}\right\}, \tag{17}$$

where $W_{\ell 0 p(2p-\ell)}$ are trigonometric functions having the pericentre as their argument and $n = \sqrt{GM/a^3}$ is the unperturbed Keplerian mean motion. Contrary to the case of small eccentricity satellites, in this case we will be forced to keep all the terms of order $\mathcal{O}(e^k)$ with $k > 2$ in computing the eccentricity functions for given pairs of ℓ and p. Moreover, we will need also all the non-zero eccentricity and inclination functions for a given degree ℓ, that is we will consider all the non-vanishing terms with $0 \leq p \leq \ell$. First, we will extend our calculations to the even zonals so far determined, i.e. $\ell = 2, 4, 6$. In this case,

$$W_{\ell 0 p(2p-\ell)} = \cos[(\ell - 2p)\dot{\omega}t] = \cos(q\dot{\omega}t). \tag{18}$$

It must be noted that the terms with

$$p = \frac{\ell}{2}, \ q = 0 \tag{19}$$

yield secular precessions, i.e. $W_{\ell 0 \frac{\ell}{2} 0} = 1$, while those with

$$q = 2p - \ell \neq 0 \tag{20}$$

induces harmonic signals with circular frequencies $-q\dot{\omega}$.

For the degree $\ell = 2$ the non-vanishing inclination and eccentricity functions and their derivatives are

$$F_{201} = \frac{3}{4}\sin^2 i - \frac{1}{2}. \tag{21}$$

$$\frac{dF_{201}}{di} = \frac{3}{2}\sin i \cos i. \tag{22}$$

$$G_{210} = \frac{1}{(1-e^2)^{3/2}}. \tag{23}$$

$$\frac{dG_{210}}{de} = \frac{2}{3}\frac{e}{(1-e^2)^{4/3}}. \tag{24}$$

In this case, only secular precessions occur.

For $\ell = 4$ we have

$$F_{401} = -\frac{35}{32}\sin^4 i + \frac{15}{16}\sin^2 i = F_{403}, \tag{25}$$

$$F_{402} = \frac{105}{64}\sin^4 i - \frac{15}{8}\sin^2 i + \frac{3}{8}. \tag{26}$$

$$\frac{dF_{401}}{di} = \left(-\frac{35}{8}\sin^3 i + \frac{15}{8}\sin i\right)\cos i = \frac{dF_{403}}{di}, \tag{27}$$

$$\frac{dF_{402}}{di} = \left(\frac{105}{16}\sin^3 i - \frac{15}{4}\sin i\right)\cos i. \tag{28}$$

$$G_{41-2} \;=\; \frac{3}{4}\frac{e^2}{(1-e^2)^{7/2}} \;=\; G_{432}, \tag{29}$$

$$G_{420} \;=\; \frac{1+\frac{3}{2}e^2}{(1-e^2)^{7/2}}. \tag{30}$$

$$\frac{dG_{41-2}}{de} \;=\; \frac{3}{14}\frac{e\,(7-6e^2)}{(1-e^2)^{8/7}} \;=\; \frac{dG_{432}}{de}, \tag{31}$$

$$\frac{dG_{420}}{de} \;=\; \frac{1}{7}\frac{e\,(23-18e^2)}{(1-e^2)^{8/7}} \tag{32}$$

In addition to secular terms, also harmonic signals with the frequencies $\pm 2\dot{\omega}$ are present.

In the case of $\ell = 6$ the inclination and eccentricity functions, along with their derivatives, are

$$F_{601} \;=\; \frac{693}{512}\sin^6 i - \frac{315}{256}\sin^4 i \;=\; F_{605}, \tag{33}$$

$$F_{602} \;=\; -\frac{3465}{1024}\sin^6 i + \frac{315}{64}\sin^4 i - \frac{105}{64}\sin^2 i \;=\; F_{604}, \tag{34}$$

$$F_{603} \;=\; \frac{1155}{256}\sin^6 i - \frac{945}{64}\sin^4 i + \frac{105}{32}\sin^2 i - \frac{5}{16}. \tag{35}$$

$$\frac{dF_{601}}{di} \;=\; \left(\frac{2079}{256}\sin^5 i - \frac{315}{64}\sin^3 i\right)\cos i \;=\; \frac{dF_{605}}{di}, \tag{36}$$

$$\frac{dF_{602}}{di} \;=\; \left(-\frac{10395}{512}\sin^5 i + \frac{315}{16}\sin^3 i - \frac{105}{32}\sin i\right)\cos i \;=\; \frac{dF_{604}}{di}, \tag{37}$$

$$\frac{dF_{603}}{di} \;=\; \left(\frac{3465}{128}\sin^5 i - \frac{945}{16}\sin^3 i + \frac{105}{16}\sin i\right)\cos i. \tag{38}$$

$$G_{61-4} = \frac{5}{16}\frac{e^4}{(1-e^2)^{11/2}} = G_{654}, \tag{39}$$

$$G_{62-2} = \frac{5}{2}\frac{e^2}{(1-e^2)^{11/2}}\left(1+\frac{e^2}{8}\right) = G_{642}, \tag{40}$$

$$G_{630} = \frac{1}{(1-e^2)^{11/2}}\left(1+5e^2+\frac{15}{8}e^4\right). \tag{41}$$

$$\frac{dG_{61-4}}{de} = \frac{5}{4}\frac{e^3\left(1-\frac{21}{22}e^2\right)}{(1-e^2)^{12/11}} = \frac{dG_{654}}{de}, \tag{42}$$

$$\frac{dG_{62-2}}{de} = 5\frac{e\left(1-\frac{29}{44}e^2-\frac{21}{88}e^4\right)}{(1-e^2)^{12/11}} = \frac{dG_{642}}{de}, \tag{43}$$

$$\frac{dG_{630}}{de} = \frac{7}{44}\frac{e\left(64-10e^2-45e^4\right)}{(1-e^2)^{12/11}}. \tag{44}$$

In addition to the secular rates, also harmonic signals with frequencies $\pm 4\dot\omega, \pm 2\dot\omega$ are present.

Let us, now, focus on the action of the odd ($\ell = 3, 5, 7, ...$) zonal ($m = 0$) harmonics. In this case,

$$W_{\ell 0p(2p-\ell)} = \sin[(\ell - 2p)\dot\omega t] = -\sin(q\dot\omega t), \tag{45}$$

so that only harmonic terms occur for $q \neq 0$.

For $\ell = 3$ we have

$$F_{301} = \frac{15}{16}\sin^3 i - \frac{3}{4}\sin i = -F_{302}, \tag{46}$$

$$\frac{dF_{301}}{di} = \left(\frac{45}{16}\sin^2 i - \frac{3}{4}\right)\cos i = -\frac{dF_{302}}{di}. \tag{47}$$

$$G_{31-1} = \frac{e}{(1 - e^2)^{5/2}} = G_{321}, \tag{48}$$

$$\frac{dG_{31-1}}{de} = \frac{1 - \frac{3}{5}e^2}{(1 - e^2)^{6/5}} = \frac{dG_{321}}{de}. \tag{49}$$

Thus, we have long-period effects varying with the frequencies $\pm\dot\omega$.

Concerning the even and odd zonal long-period harmonic terms, it must be noted that they can be approximated by secular precessions with a high level of accuracy over the expected 1-yr lifetime T of Juno because the period of its periJove is of the order of ≈ 500 yr, i.e.

$$\cos(q\omega) = \cos(q\dot\omega t + q\omega_0) \approx \cos(q\omega_0), \ 0 \le t \le T, \tag{50}$$

$$\sin\omega = \sin(\dot\omega t + \omega_0) \approx \sin\omega_0, \ 0 \le t \le T. \tag{51}$$

Thus, the choice of the initial condition ω_0 will be crucial in determining their impact.

Now, it would be possible, in principle, to use the node of Juno to measure the gravito-magnetic effect. Indeed, the Lense-Thirring node precession is independent of i, while all the zonal precessions of Ω vanish for $i = 90$ deg. It does not occur for the periJove and the mean anomaly, but they are not affected by the gravito-magnetic force for $i = 90$ deg. In reality, the situation will be likely different because of the unavoidable

orbit injection errors which will induce some departures δi of the Juno's orbital plane from the ideal polar configuration. Thus, unwanted, corrupting node zonal secular precessions will appear; their mis-modeling due to the uncertainties δJ_ℓ may swamp the recovery of the Lense-Thirring effect if their determination by Juno will not be accurate enough. Note that there is no risk of some sort of a-priori 'imprint' effect of the Lense-Thirring effect itself on the values of the zonals retrieved from the Juno's periJove motion because the gravito-magnetic pericenter precession vanishes for polar orbits.

By assuming the values quoted in Table 2 for the uncertainties δJ_ℓ, $\ell = 2, 3, 4, 6$, let us see what is the impact of a non-perfectly polar orbital geometry on the node Lense-Thirring precessions. The results are depicted in Figure 1 for each degree ℓ separately; the initial condition $\omega_0 = 90$ deg has been used. It should be noted that, in view of the likely correlations among the determined zonals, a realistic upper bound of the total bias due to them can be computed by taking the linear sum of each mis-modeled terms. The major source of bias is the so far poorly known J_6; an improvement of four orders of magnitude, which sounds rather unlikely to be obtained even with Juno (Anderson et al. 2004), would be required to push its aliasing effect at a percent level of the Lense-Thirring effect. The situation for the other zonals is more favorable; J_4 should be known better than now by a factor 1000, which is, instead, a realistic goal according to Anderson et al. (2004). Thus, we conclude that a nearly-polar orbit 1 deg off the ideal 90 deg case would likely prevent to obtain a measurement of the gravito-magnetic node precession at a decent level of accuracy.

Thanks to the high eccentricity of the Juno's orbit, also the periJove and the mean anomaly are well defined, so that they can be used in a suitable way to remove the bias of
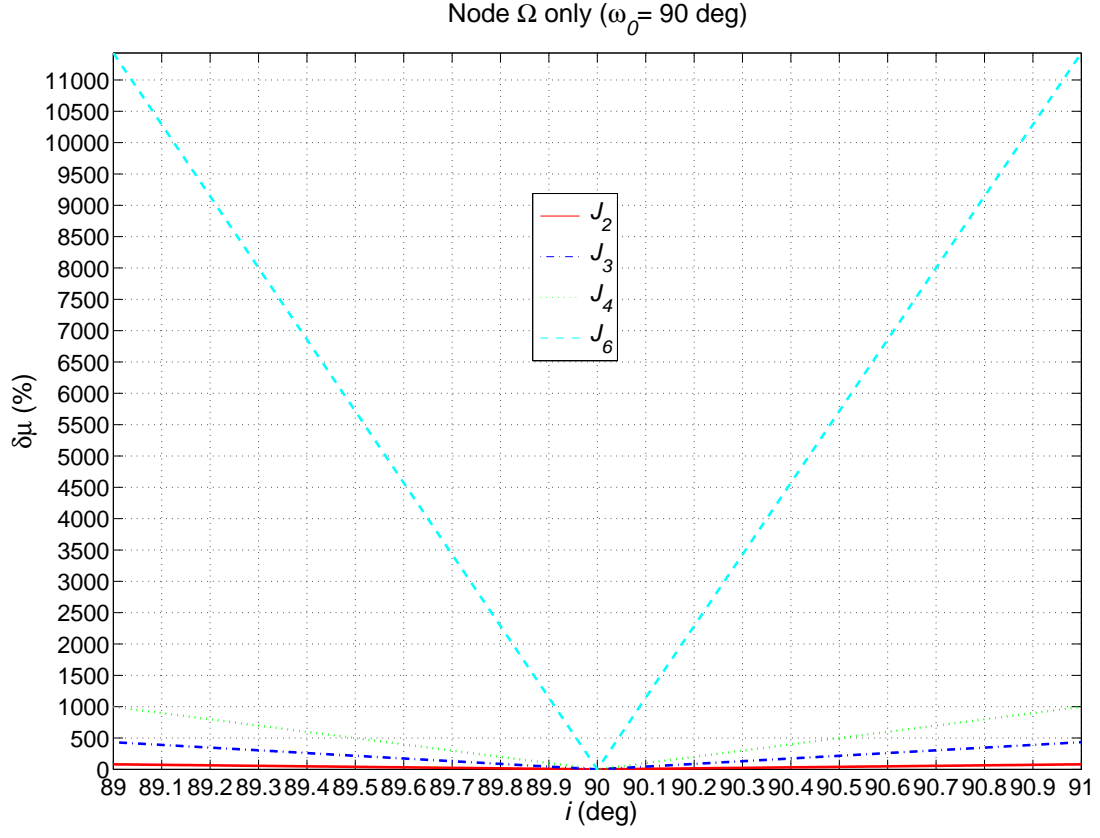
Fig. 1.— Systematic percent bias on the Lense-Thirring node precession induced by the mis-modeling in the zonals J_2, J_3, J_4, J_6 according to Table 2 for 89 deg $\leq i \leq$ 91 deg and $\omega_0 = 90$ deg.

J_6 and J_2. Let us write down

$$\delta\dot{\Omega} = \dot{\Omega}_{.2}\delta J_2 + \dot{\Omega}_{.6}\delta J_6 + \mu\dot{\Omega}_{\mathrm{LT}} + \Delta_\Omega, \tag{52}$$

$$\delta\dot{\omega} = \dot{\omega}_{.2}\delta J_2 + \dot{\omega}_{.6}\delta J_6 + \mu\dot{\omega}_{\mathrm{LT}} + \Delta_\omega, \tag{53}$$

$$\delta\dot{\mathcal{M}} = \dot{\mathcal{M}}_{.2}\delta J_2 + \dot{\mathcal{M}}_{.6}\delta J_6 + \Delta_{\mathcal{M}}. \tag{54}$$

Here $\delta\dot{\Psi}$ denotes some sort of Observed-minus-Calculated $(O - C)$ quantity for the rate of the Keplerian element Ψ which accounts for every unmodeled/mis-modeled dynamical effects; it may be, for example, a correction to the modeled precessions to be phenomenologically estimated as a solve-for parameter of a global fit of the Juno's data, or it could be a computed time-series of[6] "residuals" of Ψ by suitably overlapping orbital arcs. The gravito-magnetic force should be purposely not modeled in order to be fully present in $\delta\dot{\Psi}$. The parameter μ is[7] 1 in GTR and 0 in Newtonian mechanics and accounts for the Lense-Thirring effect. The Δ terms include all the other systematic errors like the precessions induced by the mis-modeled parts of the second even zonal harmonic δJ_4 and the first odd zonal harmonic δJ_3, the mis-modeling due to the uncertainty in Jupiter's GM, etc. By solving for μ one obtains

$$\delta\dot{\Omega} + c_1\delta\dot{\omega} + c_2\delta\dot{\mathcal{M}} = \dot{\Omega}_{\mathrm{LT}} + c_1\dot{\omega}_{\mathrm{LT}} + \Delta, \tag{55}$$

---

[6]Since the Keplerian elements are not directly measurable quantities, we use here the term "residual" in an improper sense.

[7]It is not one of the standard PPN parameters, but it can be expressed in terms of γ as $\mu = (1 + \gamma)/2$.

with

$$c_1 = \frac{\dot{\mathcal{M}}_{.6}\,\dot{\Omega}_{.2} - \dot{\Omega}_{.6}\,\dot{\mathcal{M}}_{.2}}{\dot{\omega}_{.6}\,\dot{\mathcal{M}}_{.2} - \dot{\mathcal{M}}_{.6}\,\dot{\omega}_{.2}}, \qquad (56)$$

$$c_2 = \frac{\dot{\Omega}_{.6}\,\dot{\omega}_{.2} - \dot{\omega}_{.6}\,\dot{\Omega}_{.2}}{\dot{\omega}_{.6}\,\dot{\mathcal{M}}_{.2} - \dot{\mathcal{M}}_{.6}\,\dot{\omega}_{.2}}. \qquad (57)$$

The combination of eq. (55), with eq. (56) and eq. (57), is designed, by construction, to single out the combined Lense-Thirring precessions and to cancel out the combined secular[8] precessions due to J_2 and J_6 along with their mis-modeling. Instead, it is affected by Δ which acts as a systematic bias on the Lense-Thirring signal of interest. Δ globally includes the mis-modeled part of the combined precessions induced by J_3 and J_4; the sources of uncertainty reside in J_3 and J_4 themselves and in the Jupiter's GM through the mean motion n which enters the coefficients $\dot{\Omega}_{.\ell}, \dot{\omega}_{.\ell}, \dot{\mathcal{M}}_{.\ell}$.

In Figure 2 the impact of the mis-modeling in J_3 and J_4 for $\omega_0 = 90$ deg is depicted. In Figure 3 we use $\omega_0 = 0$ deg. In this case the situation is much more favorable because for a total departure of ± 1 deg from $i = 90$ deg, an improvement of only two orders of magnitude in J_3, which is, today, still compatible with zero, and J_4 would be needed to reach the percent level; let us recall that the expected improvement in J_4 with respect to the results by Jacobson (2003) is of three orders of magnitude (Anderson et al. 2004). Note that a value of ω_0 far from 90 deg is preferable to minimize the perturbations.

Another potential source of systematic error is the Jupiter's GM whose uncertainty $\delta(GM)$ indirectly affects eq. (55) through the Keplerian mean motion n entering the uncanceled J_3 and J_4 combined precessions; δn is also present via the mean anomaly itself. However, it turns out that it is of no concern because, according to the present-day level of

---

[8]We include in them also the long-period harmonic terms for the reasons explained before.
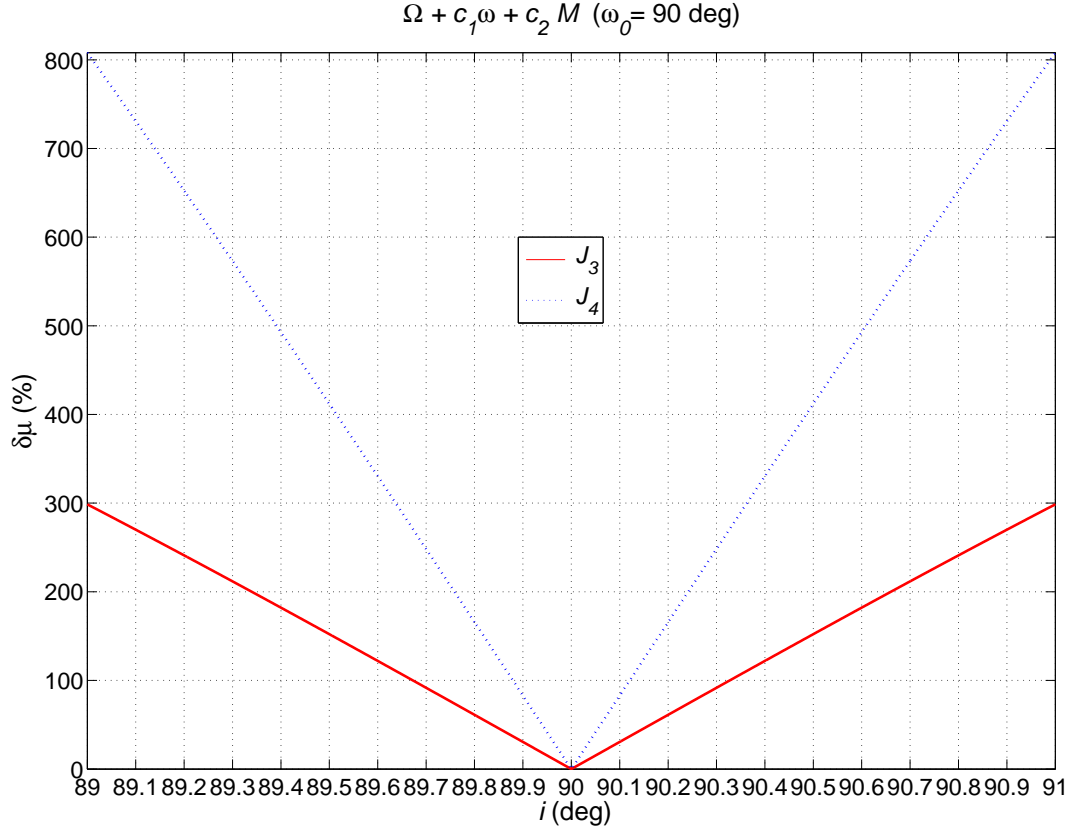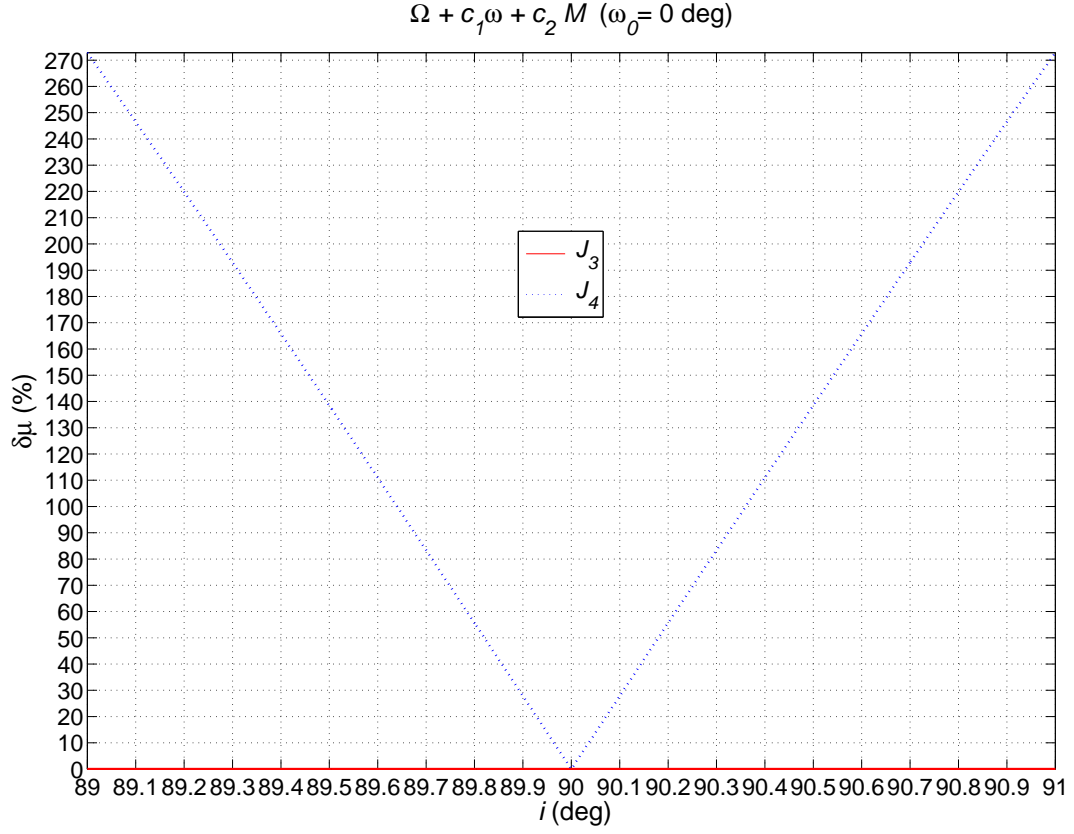
Fig. 2.— Systematic percent bias on the Lense-Thirring precessions, combined according to eq. (55), induced by the mis-modeling in the uncanceled zonals J_3, J_4 (Table 2) for 89 deg $\leq i \leq$ 91 deg and $\omega_0 = 90$ deg.

Fig. 3.— Systematic percent bias on the Lense-Thirring precessions, combined according to eq. (55), induced by the mis-modeling in the uncanceled zonals J_3, J_4 (Table 2) for 89 deg $\leq i \leq$ 91 deg and $\omega_0 = 0$ deg.

relative uncertainty (Jacobson 2003)

$$\frac{\delta(GM)}{GM} = 1.6 \times 10^{-8}, \tag{58}$$

its impact on the combined Lense-Thirring precessions is well below the percent level.

2.2.   A numerical approach

Also in this case, we followed an alternative approach based on preliminary numerical simulations. We investigated the impact of the uncertainties in the first two jovian even zonals on a Juno's single six-hours pass by numerically simulating the probe's Doppler range-rate signals due to δJ_2 and δJ_4. By assuming for them values as large as 2×10^{-10} and 3×10^{-10}, respectively, it turns out that the maximum Doppler shifts are roughly $1 - 1.5$ μm s^{-1}. Moreover, and more importantly, the time-dependent patterns of the even zonals' Doppler signals are quite different from the Lense-Thirring one removing the risk of an insidious mimicking bias. Another encouraging fact is that such simulations indicate that an inclination of even 91 deg would not compromise the recovery of the gravitomagnetic signal of interest.

3.   Discussion and conclusions

The node Ω of Juno, a recently approved spacecraft aimed to orbit Jupiter along a highly eccentric ($r_{\mathrm{min}} = 1.06 R_{\mathrm{Jup}}$, $r_{\mathrm{max}} = 39 R_{\mathrm{Jup}}$), polar ($i = 90$ deg) trajectory during one year to accurately map, among other things, its gravitational field, will be displaced by the general relativistic gravito-magnetic Lense-Thirring effect by about 572 m over the entire duration of the mission.

We, first, explored the possibility of a high accuracy measurement of such an effect

by performing analytical calculations and interpreting them in a rather conservative fashion. A meter-level accuracy in determining the jovicentric orbit of Juno should not be an unrealistic goal to be reached. Equivalently, the gravito-magnetic node precession of Juno amounts to 68.5 mas yr^{-1}, while the accuracy in measuring its node and periJove precessions should be of the order of $0.5 - 1$ mas yr^{-1}, given the expected improvements in our knowledge of the departure of the jovian gravitational field from spherical symmetry. If the Juno's orbit was perfectly polar, the long-period node precessions induced by the zonal harmonics $J_\ell, \ell = 2, 3, 4, 6, ...$ of the non-spherical jovian gravitational potential would vanish, thus removing a major source of systematic alias on the Lense-Thirring secular precession. In reality, unavoidable orbit injection errors will displace the orbital plane of Juno from the ideal polar geometry; as a consequence, the mis-modeled part of the node zonal precessions would overwhelm the relativistic signal for just $\delta i = \pm 1$ deg, in spite of the expected improvements in $J_\ell, \ell = 2, 4, 6$ of three orders of magnitude. A suitable linear combination of the node, the periJove ω and the mean anomaly $\mathcal{M}$ will allow to cancel out the effect of J_2 and J_6; the remaining uncanceled J_3 and J_4 will have an impact on the Lense-Thirring combined precessions which should be reduced down to the percent level or better by the improved low-degree zonals.

Instead of looking at the cumulative, secular effects over the entire duration of the mission, we also followed an alternative approach by looking at single Doppler range-rate measurements over time spans six hours long centered on the the probe's closest approaches to Jupiter; it turned out that, in this way, the perspectives are even more favorable. We numerically simulated the characteristic Lense-Thirring pattern for a single science pass by finding a maximum value of the order of hundreds μm s^{-1}, while the expected precision level in Juno's Doppler measurements is of the order of one μm s^{-1}. Thus, by exploiting about 25 of the planned 33 total passes of the mission it would be possible to reach a measurement accuracy below the percent level. We repeated our numerical analysis also

for the Doppler range-rate signals of J_2 and J_4 by finding quite different patterns with respect to the gravito-magnetic one; moreover, for a level of mismodeling of the order of $2 - 3 \times 10^{-10}$ in such zonals the maximum value of their biasing Doppler signals is about $1 - 1.5 \ \mu\text{m s}^{-1}$. Our numerical analysis also shows that a departure from the nominal polar orbital geometry as large as 1 deg would not compromise the successful outcome of the measurement of interest, contrary to the conservative conclusions of our analytical analysis. Thus, this approach shows that there is not a high correlation between the Lense-Thirring parameter and the jovian gravity field parameters, although a covariance analysis would be needed to prove it. However, such a covariance analysis is outside the scope of the present paper.

In conclusion, the potential error in the proposed Juno Lense-Thirring measurement is between 0.2 and 5 percent. Conversely, if one assumes the existence of gravito-magnetism as predicted by general relativity, the proposed measurement can also be considered as a direct, dynamical determination of the jovian proper angular momentum S by means of the Lense-Thirring effect at the percent level.

REFERENCES

Anderson, J.D., 1976. *The gravity field of Jupiter* in *Jupiter: Studies of the Interior, Atmosphere, Magnetosphere, and Satellites* Gehrels, T. and Matthews, M.S. (eds.) (University of Arizona Press, 1976) pp. 113-121.

Anderson, J.D., Lau, E.L., Schubert, G., Palguta, J.L., 2004. Gravity Inversion Considerations for Radio Doppler Data from the JUNO Jupiter Polar Orbiter. *American Astronomical Society*, DPS meeting #36, #14.09 http://aas.org/archives/BAAS/v36n4/dps2004/158.htm

Christodoulidis, D.C., Smith, D.E., Williamson, R.G., Klosko, S.M., 1988. *J. Geophys. Res.* **93**(B6), 6216

Ciufolini, I. and Pavlis, E.C., 2004. *Nature* **431** 958

Ciufolini, I. and Pavlis, E.C., *New Astron.* **10** 636

Conklin, J.W., et al., 2008. *J. Phys. Conf. Ser.* **140**, 012001

Crosta, M.T., and Mignard, F., 2006. *Class. Quantum Grav.* **23** 4853

Cugusi, L. Proverbio, E., 1978. *Astron. Astrophys.* **69** 321

Einstein, A., 1915. *Sitzber. Kön. Preuss. Akad. Berlin* **47** 831

Everitt, C. W. F., 1974. The Gyroscope Experiment I. General Description and Analysis of Gyroscope Performance in *Proc. Int. School Phys. "Enrico Fermi" Course LVI* Bertotti, B. (ed.) (New York: New Academic Press) pp. 331-360.

Everitt, C. W. F., et al., 2009. *Space Sci. Rev.* doi:10.1007/s11214-009-9524-7

Fomalont, E.B., and Kopeikin, S.M., 2008. Radio interferometric tests of general relativity in *A Giant Step: from Milli- to Micro-arcsecond Astrometry Proceedings IAU Symposium No. 248, 2007* Jin, W.J., Platais, I., and Perryman, M.A.C. (eds.) (Cambridge University Press, 2008), pp. 383-386.

Guillot, T., 2005. *Ann. Rev. Earth Planet. Sci.* **33** 493

Haas, M. R., and Ross, D. K., 1975. *Astrophys. Space Sci.* **32** 3

Hiscock, W.A., and Lindblom, L., 1979. *Astroph. J.* **231** 224

Hori, Y., Sano, T., Ikoma, M., Ida, S., 2008. in: Sun, Y.-S., Ferraz-Mello, S., Zhou, J.-L. (eds.), *EXOPLANETS: Detection, Formation and Dynamics Proceedings IAU Symposium No. 249*, pp. 119-122.

Iorio, L., 2006. *Class. Quantum Gravit.* **23**, 5451

Iorio, L., 2007a. *Planet. Space Sci.* **55**, 503

Iorio, L. (ed.), 2007b. *The Measurement of Gravitomagnetism: A Challenging Enterprise.* (NOVA, Hauppauge)

Iorio, L., 2008. *Scholarly Research Exchange* **2008**, 105235

Iorio, L., 2009a. *Centr. Eur. J. Phys.* doi:10.2478/s11534-009-0117-6

Iorio, L., 2009b. *Centr. Eur. J. Phys.* **8**, 25

Iorio, L., 2009c. *Adv. Space Res.* **43** 1148

Iorio, L., 2009d. *Gen. Relativ. Gravit.* **41** 1717

Iorio, L., and Lainey, V., 2005. *Int. J. Mod. Phys. D* **14**, 2039

Irwin, P., 2003. *Giant Planets of Our Solar System* (Springer)

Jacobson, R.A., 2003. JUP230 orbit solution

Kaula, W.M., 1966. Theory of Satellite Geodesy (Blaisdell, Waltham)

Krogh, K., 2007. *Class. Quantum Grav.* **24**, 5709

Lense, J. and Thirring, H., 1918. *Phys. Z.* **19** 156 Translated and discussed in Mashhoon, B., Hehl, F.W., Theiss, D.S., 1984. *Gen. Relativ. Gravit.* **16** 711. Reprinted in Ruffini, R.J., Sigismondi, C. (eds), 2003. *Nonlinear Gravitodynamics* (Singapore: World Scientific) pp 349–88,

Lichtenegger, H.I.M. and Iorio, L., 2007. *Post-Newtonian Orbital Perturbations* in Iorio L (ed.) *The Measurement of Gravitomagnetism: A Challenging Enterprise* (Hauppauge, New York: NOVA publishers) pp. 87-100.

Machida, M.N., Kokubo, E., Inutsuka, S., Matsumoto, T., 2008. *Astroph. J.* **685** 1220

Mashhoon, B., 2007. *Gravitoelectromagnetism: A Brief Review* in Iorio, L. (ed.) *The Measurement of Gravitomagnetism: A Challenging Enterprise* (Hauppauge, New York: NOVA publishers) pp. 29-39.

Matousek, S, 2007. *Acta Astronautica* **61** 932

Pugh, G.E., 1959. WSEG Research Memorandum No. 11

Ries, J.C., Eanes, R.J., Watkins, M.M., 2008. Confirming the Frame-Dragging Effect with Satellite Laser Ranging 16th Int. Laser Ranging Workshop, (Poznań (PL) 13-17 October 2008).

Schiff, L., 1960. *Phys. Rev. Lett.* **4** 215

Soffel, M., 1989. *Relativity in Astrometry, Celestial Mechanics and Geodesy* (Berlin: Springer)

Soffel, M., Klioner, S.A., Petit, G., et al., 2003. *Astron. J.* **126**, 2687

Zel'dovich, Ya.B., Novikov, I.D., 1971. *Stars and Relativity* (Chicago: The University of Chicago Press)